

Supporting Information

Isolation of copper photocatalyst on metal–organic cage for the sulfonylation of aryl halides by visible-light mediated C(sp²)–sulfur cross-coupling

Lehua Zhao,^{+a} Yu Zhang,^{+a} Huali Wang,^a Jing Wang,^a Cheng He,^a Liang Zhao,^{a*} and Chunying Duan^b

^aState Key Laboratory of Fine Chemicals, Frontier Science Center for Smart Materials, Dalian University of Technology, Dalian 116024, P. R. China.

^bState Key Laboratory of Coordination Chemistry, Nanjing University, Nanjing 210093, P. R. China.

⁺These authors contributed equally to this work.

Corresponding Author.

*Email address: zhaol@dlut.edu.cn

Contents

1. Experimental Section.
2. Preparation and Characterizations.
3. Single Crystal X-ray Crystallography.
4. ESI-MS Spectra.
5. Data for Interaction between Cu^I ions and Ce–BPDS.
6. Data Relative to the Photocatalytic C(sp²)–S Cross-Coupling.
7. NMR spectra.
8. References.

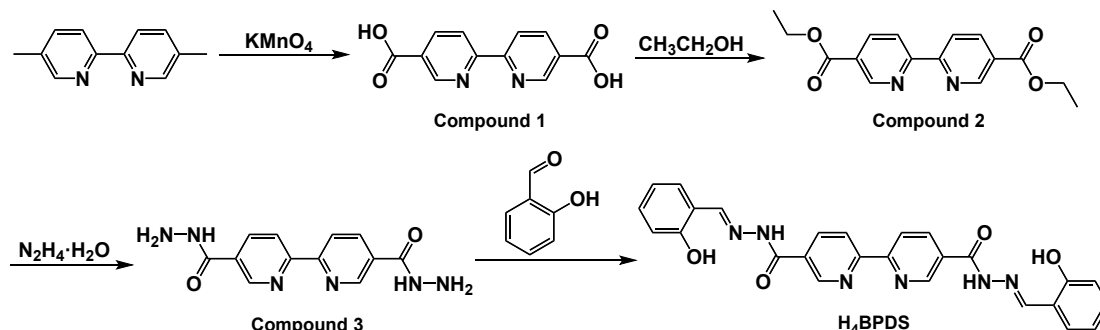
1. Experimental Section.

All the chemicals and solvents were of reagent grade quality obtained from commercial sources and used without further purification. The elemental analyses of C, H and N were performed on an Elementar UNICUBE elemental analyzer. NMR spectra were measured on the Bruker Avance NEO 600 M spectrometer, Bruker Avance II 400 spectrometer, or Varian 400 M spectrometer. ESI-MS spectra were carried out on an Agilent 6224 HPLC-TOF spectrometer using methanol as the mobile phase. UV-Vis absorption spectra were recorded on a PERSEE T9CS spectrometer. The fluorescent spectra were measured on Edinburgh FLS1000 stable/transient fluorescence spectrometer. Thermogravimetric analyses (TGA) were recorded on a TA Q500 thermogravimeter from 20 to 800 °C at a rate of 10 °C/min under a nitrogen atmosphere. Energy-dispersive system elemental mapping images were obtained on a JEOL JSM-7610F Plus Field Emission Scanning Electron Microscopy. Fourier transform infrared (FT-IR) spectra were recorded using KBr pellets on a ThermoFisher 6700. X-ray photoelectron spectroscopy (XPS) signals were collected on a Thermo ESCALAB Xi+ spectrometer. Isothermal Titration Calorimetry (ITC) was performed on a Nano ITC (TA Instruments Inc. — Waters LLC). Cyclic voltammetry (CV) was performed on a ZAHNER ENNIUM electrochemical workstation, after degassing the solutions with argon, with a conventional three-electrode system using an Ag/AgCl electrode as the reference electrode, 0.5 mm diameter platinum silk as the counter electrode, and a glassy carbon electrode as the working electrode. The light source is 395 nm LED which was purchased from the Beijing China Education Au-light Co. Ltd. The gas chromatography (GC) analyses were performed on an Agilent Technologies 7890B GC system.

For photocatalytic C(sp²)-S cross-coupling, each sample was made in a 15 mL flame-dried Schlenk quartz flask. As the standard method, the Ce-**BPDS** (0.5 μmol), CuI (1.0 μmol), substrate **1** (0.05 mmol), substrate **2** (0.5 mmol), and Cs₂CO₃ (0.05 mmol) in DMSO were added to obtain a total volume of 2.0 mL. The flask was sealed with a septum and protected from air, then degassed by bubbling argon gas for 15 min under atmospheric pressure at room temperature. After that, the samples were irradiated by a 395 nm of LED, and the reaction temperature was 298K by using a fan to dissipate heat. After irradiation, 1,3,5-trimethoxybenzene (0.05 mmol, the same amount as the substrate **1**) was added to reaction solution. And then, the solution was carried out by GC analysis. The GC program was set to heat from 60 °C to 300 °C (15 °C/min). The response time of the 1,3,5-trimethoxybenzene signal is around 10.5 minutes. The response time of the catalytic product signals are in the range of 14.0-18.0 minutes. The yields of all products were obtained by calculating the ratio of peak areas between products and 1,3,5-trimethoxybenzene.

2. Preparation and Characterizations.

Scheme 1. The synthetic routes of the H₄BPDS.



Synthesis of compound 1

Potassium permanganate (8.22 g, 52 mmol) and 5,5'-dimethyl-2,2'-bipyridine (1.47 g, 8 mmol) in H₂O (60 mL) were stirred and heated at 115°C for 2 h.^{S1} The mixture was cooled to room temperature and filtered through celite. The filtrate was acidified with concentrated hydrochloric acid until precipitation of a white solid, which was filtrated, washed with water, and dried to afford the desired product. Yield: 1.81 g, 93%. ¹H NMR (400 MHz, DMSO-*d*₆): δ 13.53 (s, 2H), 9.21 (s, 2H), 8.59 (d, *J* = 8.0 Hz, 2H), 8.46 (d, *J* = 8.0 Hz, 2H).

Synthesis of compound 2

Compound 1 (1.71 g, 7 mmol) was suspended in 100 mL of absolute ethanol. Concentrated sulfuric acid (2.0 mL) was slowly added and the resulting mixture was stirred and refluxed for 18 h.^{S1} The mixture was cooled to room temperature and neutralized with the saturated NaHCO₃ solution until pH=7. It was then poured into water (200 mL) and extracted with dichloromethane (3 × 50 mL). The combined organic layers were dried over Na₂SO₄ and filtered. Evaporation of the filtrate and evaporate under vacuum to obtain a white solid. Yield:

1.81 g, 86%. $^1\text{H NMR}$ (400 MHz, CDCl_3): δ 9.29 (s, 2H), 8.58 (d, $J = 8.4$ Hz, 2H), 8.44 (d, $J = 8.4$ Hz, 2H), 4.45 (q, $J = 3.2$ Hz, 4H), 1.44 (t, $J = 3.2$ Hz, 6H).

Synthesis of compound 3

Compound 2 (1.80 g, 6 mmol) was added to an ethanol (80 mL) containing 80% hydrazine hydrate (1.2 g, 24 mmol), and the resultant mixture was stirred and refluxed for 24 h.^{S2} The white solid was collected by filtration, washed with ethanol and dried in vacuum. Yield: 1.39 g, 85%. $^1\text{H NMR}$ (600 MHz, $\text{DMSO}-d_6$): δ 10.08 (s, 2H), 9.09 (s, 2H), 8.50 (d, $J = 8.4$ Hz, 2H), 8.34 (d, $J = 8.4$ Hz, 2H), 4.66 (s, 4H).

Synthesis of H_4BPDS

Compound 3 (1.36 g, 5 mmol) and salicylaldehyde (1.22 g, 10 mmol) were mixed in methanol (60 mL). After 3 drops of acetic acid were added, the mixture was stirred and refluxed for 24 h. After the reaction cooled down, the white solid was collected by filtration, washed with methanol and dried in vacuum. Yield: 1.80 g, 75%. $^1\text{H NMR}$ (600 MHz, $\text{DMSO}-d_6$): δ 12.35 (s, 2H), 11.14 (s, 2H), 9.25 (s, 2H), 8.70 (s, 2H), 8.63 (d, $J = 8.4$ Hz, 2H), 8.50 (d, $J = 8.4$ Hz, 2H), 7.62 (d, $J = 6.6$ Hz, 2H), 7.33 (t, $J = 7.8$ Hz, 2H), 6.95 (dd, $J = 12.0, 7.8$ Hz, 4H). $^{13}\text{C NMR}$ (101 MHz, $\text{DMSO}-d_6$): δ 161.6, 157.9, 157.2, 149.3, 149.0, 137.4, 132.2, 129.7, 129.6, 121.3, 119.9, 119.2, 116.9. **Elemental analysis:** calcd for $\text{C}_{26}\text{H}_{20}\text{N}_6\text{O}_4$: H, 4.20%; C, 64.98%; N, 17.50%; Found: H, 4.38%; C, 64.92%; N, 17.48%. **ESI-MS:** calcd for $\text{C}_{26}\text{H}_{20}\text{N}_6\text{O}_4$: 480.1546; Found: 479.1473 $[\text{M}-\text{H}]^-$.

Preparation of Ce-BPDS

A solution of $\text{Ce}(\text{NO}_3)_3 \cdot 6\text{H}_2\text{O}$ (52.1 mg, 0.12 mmol), H_4BPDS (48 mg, 0.1 mmol) and NaOH (8 mg, 0.2 mmol) in $\text{CH}_3\text{OH}/\text{DMF}$ (v:v = 1.5:10, 11.5 mL) was stirred for 2 h. X-ray quality black block crystals were obtained after the solution left for several weeks at room temperature. Yield: 62%. **Elemental analysis:** calcd for $\text{Ce}_4(\text{C}_{26}\text{H}_{18}\text{N}_6\text{O}_4)_6 \cdot 3(\text{C}_3\text{H}_7\text{NO})$: H, 3.56%; C, 54.28%; N, 14.96%; Found: H, 3.68%; C, 54.12%; N, 14.88%. **ESI-MS:** m/z : 857.6121 [$\text{Ce}_4(\text{H}_2\text{BPDS})_6$] $^{4+}$ and 1143.1476 [$\text{Ce}_4(\text{H}_2\text{BPDS})_5(\text{HBPDS})$] $^{3+}$.

3. Single Crystal X-ray Crystallography.

Intensity of the Ce-BPDS was collected on a Bruker SMART APEX CCD diffractometer with graphite monochromated $\text{Mo-K}\alpha$ ($\lambda = 0.71073 \text{ \AA}$) using the SMART and SAINT programs.^{S3,S4} The structure was solved by Intrinsic Phasing using SHELXT and refined by Least Squares minimization using SHELXL in OLEX2.^{S5-S7} Non-H atoms were refined with anisotropic displacement parameters. Hydrogen atoms in the backbones were fixed geometrically at calculated distances and allowed to ride on the parent non-hydrogen atoms, whereas some of the disordered solvent molecules were not treated during the structural refinements. The SQUEEZE program was carried out for Ce-BPDS .^{S8}

Table S1. Crystallographic data for Ce–BPDS.

Compound	Ce–BPDS
Formula	$\text{Ce}_4(\text{C}_{26}\text{H}_{18}\text{N}_6\text{O}_4)_6 \cdot 3(\text{C}_3\text{H}_7\text{NO})$
M ($\text{g} \cdot \text{mol}^{-1}$)	3650.54
Crystal system	Triclinic
Space group	$P\bar{1}$
a (\AA)	22.747(2)
b (\AA)	25.744(3)
c (\AA)	26.168(2)
V (\AA^3)	13601(2)
Z	2
D_{calcd} ($\text{g} \cdot \text{cm}^{-3}$)	0.891
F (000)	3680
μ (mm^{-1})	0.706
T (K)	219
Refl. collected/unique	299733/62422 [$R_{\text{int}} = 0.0866$]
R_1 [$I > 2\sigma(I)$]	0.0634
wR_2 (all data)	0.2001
Goodness of fit	1.032
Max/min $\Delta\rho$ ($\text{e} \text{\AA}^{-3}$)	2.187 and -1.404
CCDC Number	2349168

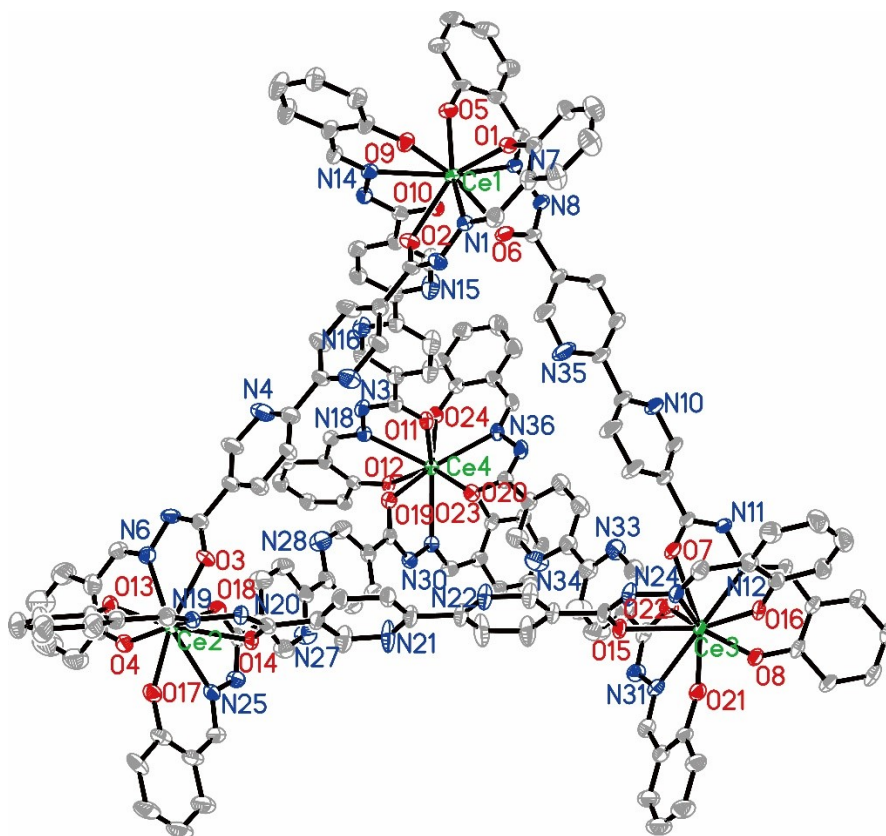


Figure S1. An ORTEP plot of the Ce-BPDS, showing 30% probability displacement ellipsoids of non-hydrogen atoms. Hydrogen atoms are omitted for clarity.

Table S2. Selective bond distance (Å) in Ce–BPDS.

Bond	Bond distance (Å)	Bond	Bond distance (Å)
Ce(1)-O(1)	2.215(3)	O(1)-C(1)	1.318(6)
Ce(1)-O(9)	2.214(3)	O(9)-C(52)	1.297(6)
Ce(1)-O(10)	2.466(3)	O(10)-C(59)	1.228(6)
Ce(1)-O(5)	2.222(3)	O(5)-C(162)	1.317(6)
Ce(1)-O(2)	2.368(3)	O(2)-C(8)	1.298(6)
Ce(1)-O(6)	2.380(3)	O(6)-C(33)	1.249(6)
Ce(1)-N(14)	2.679(4)	O(3)-C(19)	1.264(6)
Ce(1)-N(1)	2.649(4)	O(4)-C(26)	1.278(7)
Ce(1)-N(7)	2.679(4)	O(14)-C(85)	1.256(6)
Ce(2)-O(3)	2.338(3)	O(17)-C(104)	1.314(7)
Ce(2)-O(4)	2.204(4)	O(13)-C(78)	1.303(6)
Ce(2)-O(14)	2.525(3)	O(18)-C(111)	1.272(6)
Ce(2)-O(17)	2.200(4)	O(21)-C(151)	1.327(6)
Ce(2)-O(13)	2.224(3)	O(16)-C(103)	1.318(6)
Ce(2)-O(18)	2.448(3)	O(8)-C(51)	1.322(6)
Ce(2)-N(25)	2.667(4)	O(15)-C(96)	1.216(6)
Ce(2)-N(19)	2.628(4)	O(7)-C(44)	1.252(6)
Ce(2)-N(6)	2.599(4)	O(22)-C(148)	1.312(7)
Ce(3)-O(21)	2.207(3)	O(12)-C(77)	1.320(6)
Ce(3)-O(16)	2.202(4)	O(24)-C(130)	1.306(6)
Ce(3)-O(8)	2.234(3)	O(11)-C(70)	1.256(6)
Ce(3)-O(15)	2.492(3)	O(23)-C(137)	1.266(6)
Ce(3)-O(7)	2.481(3)	O(20)-C(129)	1.315(6)
Ce(3)-O(22)	2.323(3)	O(19)-C(122)	1.243(6)
Ce(3)-O(N12)	2.642(4)	N(14)-N(40)	1.381(5)
Ce(3)-O(N24)	2.703(4)	N(14)-C(58)	1.258(6)
Ce(3)-N(31)	2.618(5)	N(1)-C(7)	1.282(7)

Ce(4)-O(12)	2.212(3)	N(7)-C(32)	1.298(7)
Ce(4)-O(24)	2.203(3)	N(1)-N(2)	1.384(6)
Ce(4)-O(11)	2.459(3)	N(8)-N(7)	1.399(5)
Ce(4)-O(23)	2.384(3)	N(25)-N(26)	1.382(6)
Ce(4)-O(20)	2.224(3)	N(25)-C(110)	1.316(6)
Ce(4)-O(19)	2.490(3)	N(19)-N(20)	1.418(5)
Ce(4)-N(18)	2.659(4)	N(19)-C(84)	1.282(7)
Ce(4)-N(36)	2.633(4)	N(6)-C(20)	1.288(8)
Ce(4)-N(30)	2.672(4)	N(5)-N(6)	1.401(6)
N(12)-C(45)	1.276(6)	N(12)-N(11)	1.412(5)
N(24)-C(97)	1.277(7)	N(24)-N(23)	1.390(6)
N(31)-N(32)	1.396(6)	N(31)-C(149)	1.286(7)
N(18)-C(71)	1.293(7)	N(17)-N(18)	1.423(5)
N(36)-N(13)	1.409(6)	N(30)-N(29)	1.388(5)
N(36)-C(136)	1.280(7)	N(30)-C(123)	1.285(7)

Table S3. Selective bond angle (°) in Ce–BPDS.

Bond	Bond angle (°)	Bond	Bond angle (°)
O(1)-Ce(1)-O(9)	86.11(13)	O(5)-Ce(1)-O(10)	85.61(13)
O(1)-Ce(1)-O(10)	142.25(12)	O(5)-Ce(1)-O(2)	140.11(14)
O(1)-Ce(1)-O(5)	87.6.90(13)	O(5)-Ce(1)-O(6)	128.81(13)
O(1)-Ce(1)-O(2)	130.91(13)	O(5)-Ce(1)-N(14)	75.32(13)
O(1)-Ce(1)-O(6)	82.62(13)	O(5)-Ce(1)-N(1)	149.95(13)
O(1)-Ce(1)-N(14)	150.13(12)	O(5)-Ce(1)-N(7)	67.44(13)
O(1)-Ce(1)-N(1)	69.64(13)	O(2)-Ce(1)-O(10)	71.37(12)
O(1)-Ce(1)-N(7)	78.56(13)	O(2)-Ce(1)-O(6)	76.09(13)
O(9)-Ce(1)-O(10)	129.59(12)	O(2)-Ce(1)-N(14)	65.13(13)
O(9)-Ce(1)-O(5)	83.91(14)	O(2)-Ce(1)-N(1)	61.45(13)
O(9)-Ce(1)-O(2)	86.36(13)	O(2)-Ce(1)-N(7)	124.80(12)
O(9)-Ce(1)-O(6)	144.36(13)	O(6)-Ce(1)-O(10)	73.73(13)
O(9)-Ce(1)-N(14)	68.54(12)	O(6)-Ce(1)-N(14)	127.21(13)
O(9)-Ce(1)-N(1)	76.24(13)	O(6)-Ce(1)-N(1)	68.13(12)
O(9)-Ce(1)-N(7)	147.95(13)	O(6)-Ce(1)-N(7)	61.38(11)
O(10)-Ce(1)-N(14)	61.010(11)	N(14)-Ce(1)-N(7)	114.78(12)
O(10)-Ce(1)-N(1)	124.43(12)	N(1)-Ce(1)-N(14)	116.50(12)
O(10)-Ce(1)-N(7)	64.41(12)	N(1)-Ce(1)-N(7)	122.71(12)
O(3)-Ce(2)-O(14)	70.03(12)	O(4)-Ce(2)-O(3)	131.56(13)
O(3)-Ce(2)-O(18)	76.02(13)	O(4)-Ce(2)-O(14)	139.51(13)
O(3)-Ce(2)-N(25)	123.44(13)	O(4)-Ce(2)-O(13)	89.04(14)
O(3)-Ce(2)-N(19)	66.12(12)	O(4)-Ce(2)-O(18)	80.26(13)
O(3)-Ce(2)-N(6)	61.70(14)	O(4)-Ce(2)-N(25)	77.25(14)
O(14)-Ce(2)-N(25)	63.49(13)	O(4)-Ce(2)-N(19)	152.32(13)
O(14)-Ce(2)-N(19)	61.00(12)	O(4)-Ce(2)-N(6)	70.23(14)
O(14)-Ce(2)-N(6)	122.22(13)	O(17)-Ce(2)-O(3)	140.89(14)
O(13)-Ce(2)-O(3)	88.78(13)	O(17)-Ce(2)-O(4)	86.13(14)

O(13)-Ce(2)-O(14)	129.29(13)	O(17)-Ce(2)-O(14)	87.81(13)
O(13)-Ce(2)-O(18)	147.20(13)	O(17)-Ce(2)-O(13)	80.79(14)
O(13)-Ce(2)-N(25)	146.16(13)	O(17)-Ce(2)-O(18)	128.66(13)
O(13)-Ce(2)-N(19)	68.32(13)	O(17)-Ce(2)-N(25)	67.68(13)
O(13)-Ce(2)-N(6)	80.51(14)	O(17)-Ce(2)-N(19)	75.02(13)
O(18)-Ce(2)-O(14)	72.69(12)	O(17)-Ce(2)-N(6)	149.94(15)
O(18)-Ce(2)-N(25)	60.07(12)	N(19)-Ce(2)-N(25)	112.60(13)
O(18)-Ce(2)-N(19)	127.37(13)	N(6)-Ce(2)-N(25)	121.77(13)
O(18)-Ce(2)-N(6)	66.68(13)	N(6)-Ce(2)-N(19)	118.72(14)
O(21)-Ce(3)-O(8)	89.26(13)	O(16)-Ce(3)-O(21)	86.08(13)
O(21)-Ce(3)-O(15)	79.20(12)	O(16)-Ce(3)-O(8)	79.43(13)
O(21)-Ce(3)-O(7)	139.73(12)	O(16)-Ce(3)-O(15)	126.94(12)
O(21)-Ce(3)-O(22)	132.48(14)	O(16)-Ce(3)-O(7)	89.98(13)
O(21)-Ce(3)-N(12)	150.35(12)	O(16)-Ce(3)-O(22)	139.05(13)
O(21)-Ce(3)-N(24)	80.20(13)	O(16)-Ce(3)-N(12)	71.01(13)
O(21)-Ce(3)-N(31)	70.49(13)	O(16)-Ce(3)-N(24)	66.32(13)
O(8)-Ce(3)-O(15)	149.65(13)	O(16)-Ce(3)-N(31)	149.73(13)
O(8)-Ce(3)-O(7)	129.31(12)	O(15)-Ce(3)-N(12)	129.60(11)
O(8)-Ce(3)-O(22)	86.87(14)	O(15)-Ce(3)-N(24)	61.05(12)
O(8)-Ce(3)-N(12)	68.66(12)	O(15)-Ce(3)-N(31)	68.39(13)
O(8)-Ce(3)-N(24)	144.63(13)	O(7)-Ce(3)-O(15)	71.46(12)
O(8)-Ce(3)-N(31)	81.32(13)	O(7)-Ce(3)-N(12)	61.07(11)
O(22)-Ce(3)-O(15)	80.79(13)	O(7)-Ce(3)-N(24)	61.74(12)
O(22)-Ce(3)-O(7)	69.45(13)	O(7)-Ce(3)-N(31)	120.29(13)
O(22)-Ce(3)-N(12)	68.06(13)	N(12)-Ce(3)-N(24)	106.11(13)
O(22)-Ce(3)-N(24)	124.81(13)	N(31)-Ce(3)-N(12)	122.38(13)
O(22)-Ce(3)-N(31)	62.10(13)	N(31)-Ce(3)-N(24)	125.10(13)
O(12)-Ce(4)-O(11)	129.30(12)	O(24)-Ce(4)-O(12)	85.53(13)
O(12)-Ce(4)-O(23)	141.90(13)	O(24)-Ce(4)-O(11)	82.31(13)

O(12)-Ce(4)-O(20)	87.44(13)	O(24)-Ce(4)-O(23)	131.13(13)
O(12)-Ce(4)-O(19)	85.65(12)	O(24)-Ce(4)-O(20)	87.66(13)
O(12)-Ce(4)-N(18)	67.78(12)	O(24)-Ce(4)-O(19)	141.43(12)
O(12)-Ce(4)-N(36)	148.53(12)	O(24)-Ce(4)-N(18)	77.57(13)
O(12)-Ce(4)-N(30)	75.83(13)	O(24)-Ce(4)-N(36)	69.43(13)
O(11)-Ce(4)-O(19)	74.69(12)	O(24)-Ce(4)-N(30)	149.74(13)
O(11)-Ce(4)-N(18)	61.54(12)	O(23)-Ce(4)-O(11)	74.04(13)
O(11)-Ce(4)-N(36)	67.47(12)	O(23)-Ce(4)-O(19)	71.26(12)
O(11)-Ce(4)-N(30)	127.92(12)	O(23)-Ce(4)-N(18)	123.10(12)
O(20)-Ce(4)-O(11)	140.52(12)	O(23)-Ce(4)-N(36)	62.13(13)
O(20)-Ce(4)-O(23)	84.64(13)	O(23)-Ce(4)-N(30)	66.59(13)
O(20)-Ce(4)-O(19)	129.30(12)	O(19)-Ce(4)-N(18)	64.35(12)
O(20)-Ce(4)-N(18)	151.82(13)	O(19)-Ce(4)-N(36)	125.81(12)
O(20)-Ce(4)-N(36)	73.24(13)	O(19)-Ce(4)-N(30)	61.44(12)
O(20)-Ce(4)-N(30)	68.16(12)	N(18)-Ce(4)-N(30)	115.50(13)
N(36)-Ce(4)-N(18)	121.78(13)	N(36)-Ce(4)-N(30)	117.19(14)

4. ESI-MS Spectra.

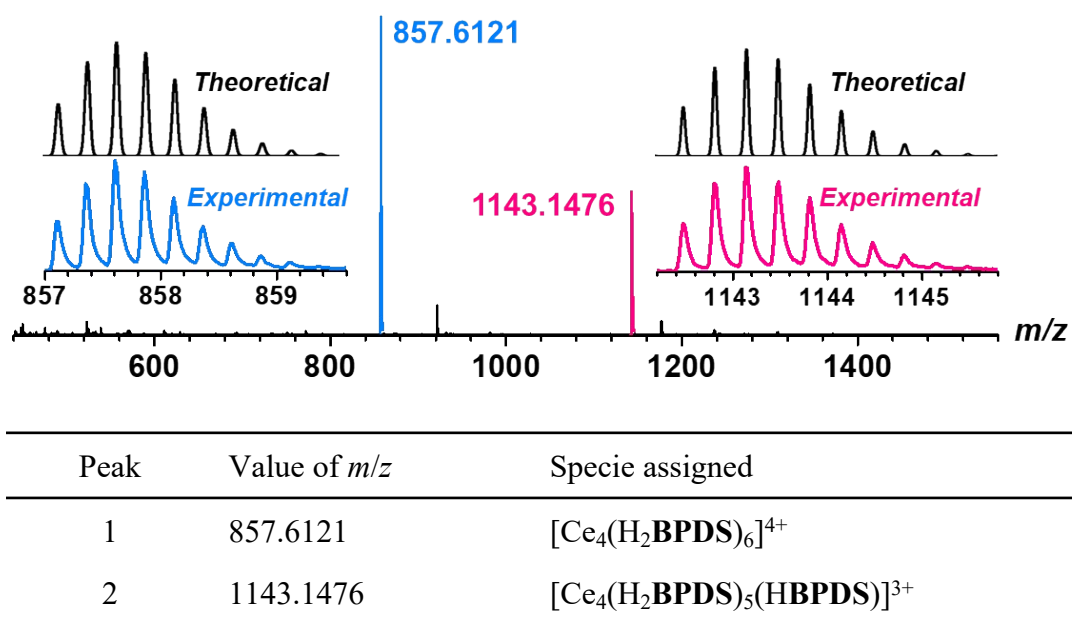
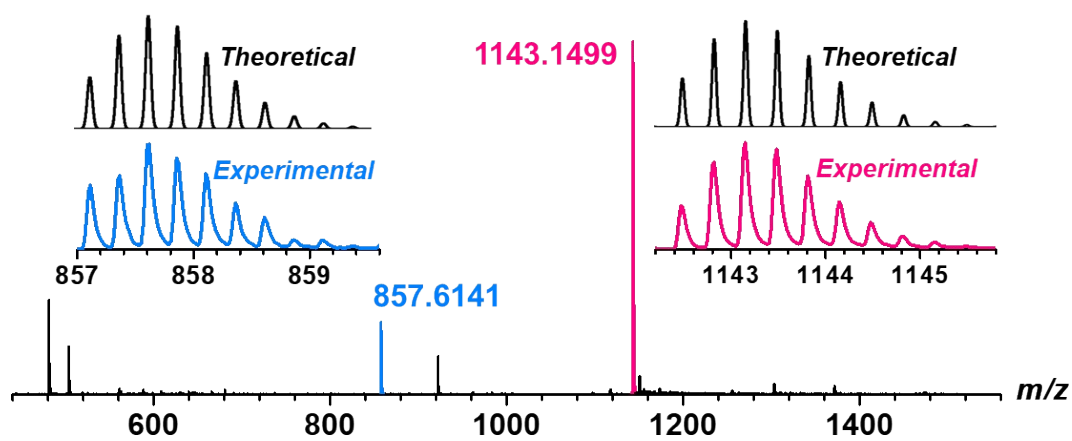


Figure S2. ESI-MS spectra of Ce-BPDS (0.1 mM) in DMSO. The inserts showed the measured and simulated isotopic patterns at $m/z = 857.6121$ and 1143.1476 , respectively.



Peak	Value of m/z	Specie assigned
1	857.6141	$[\text{Ce}_4(\text{H}_2\text{BPDS})_6]^{4+}$
2	1143.1499	$[\text{Ce}_4(\text{H}_2\text{BPDS})_5(\text{HBPDS})]^{3+}$

Figure S3. ESI-MS spectra of Ce-BPDS after reaction under standard catalytic conditions.

The inserts showed the measured and simulated isotopic patterns at $m/z = 857.6141$ and 1143.1499 , respectively.

5. Data for Interaction between Cu^{I} ions and Ce-BPDS.

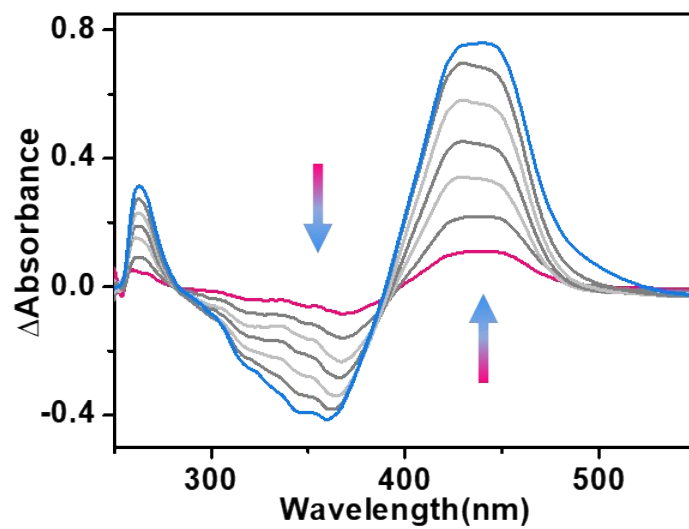


Figure S4. UV-vis absorption difference spectra of Ce-BPDS (10.0 μM) in DMSO upon the addition of CuI (30.0 μM).

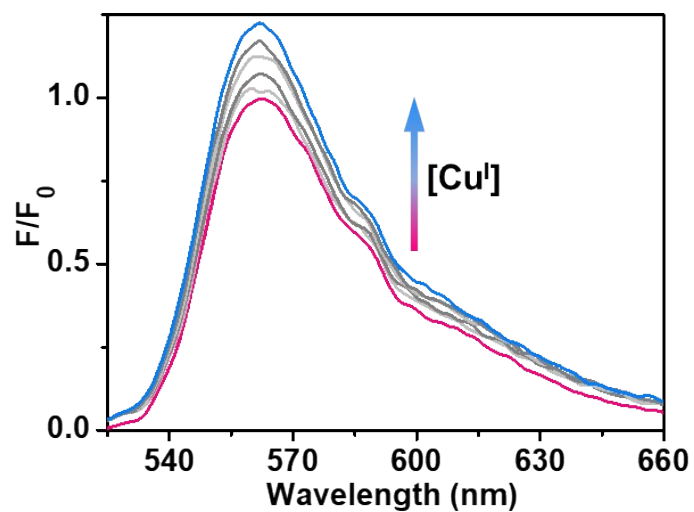


Figure S5. Luminescence spectra of Ce-BPDS (10.0 μM) in DMSO upon the addition of CuI (30.0 μM), excited at 500 nm.

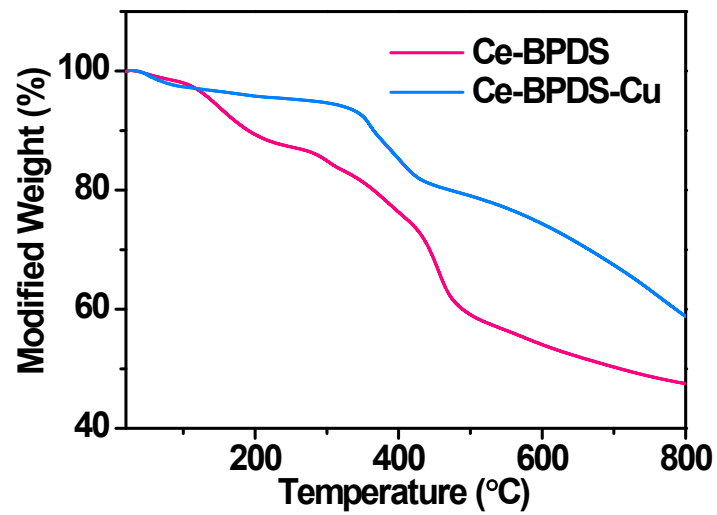


Figure S6. TGA spectra of Ce-BPDS and Ce-BPDS-Cu.

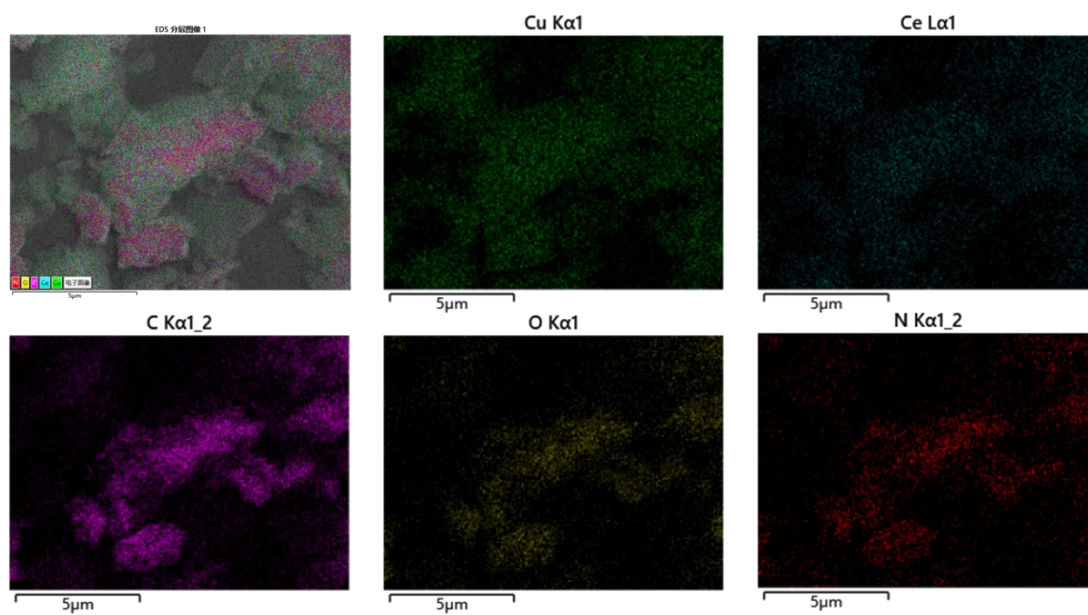


Figure S7. Scanning electron microscopy image and energy-dispersive system elemental mapping images of Ce-BPDS-Cu.

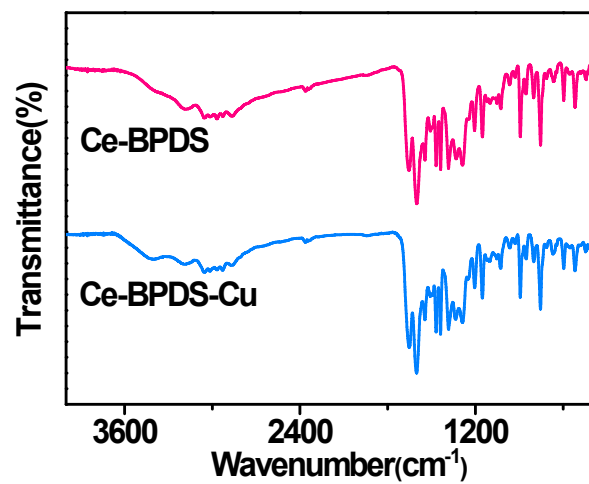


Figure S8. FT-IR spectra of Ce-BPDS and Ce-BPDS-Cu.

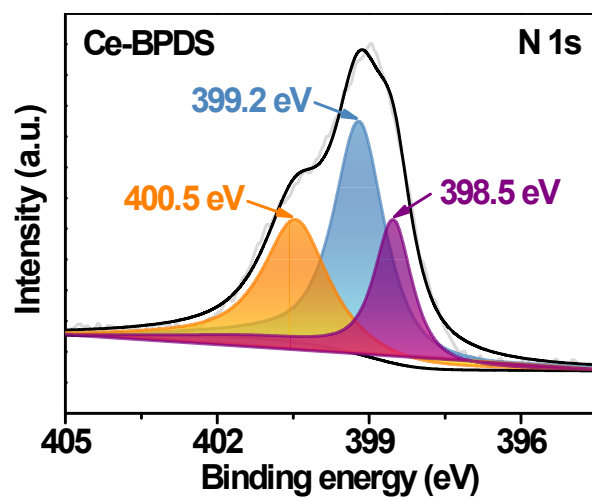


Figure S9. N 1s XPS spectra of Ce-BPDS.

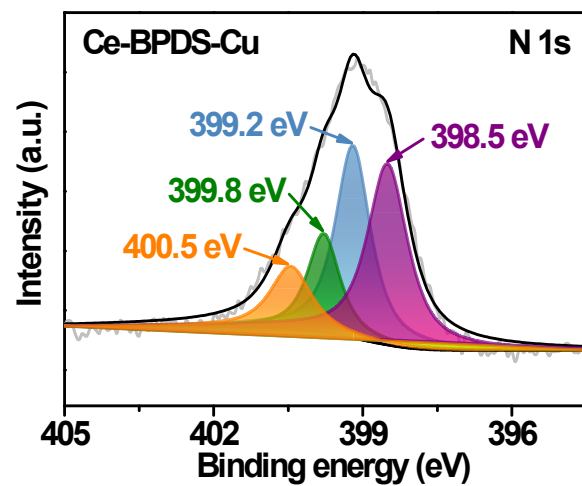


Figure S10. N 1s XPS spectra of Ce-BPDS-Cu.

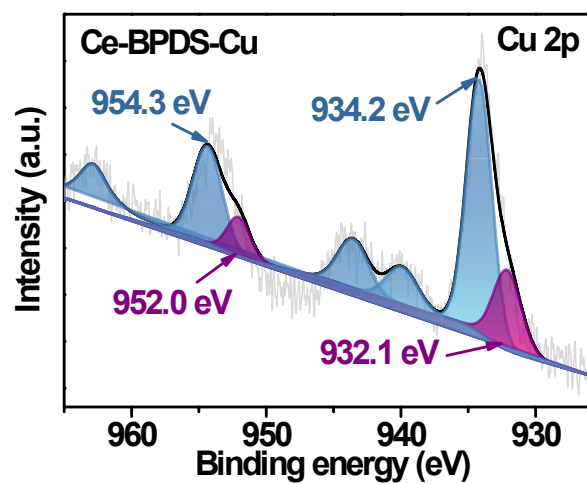


Figure S11. Cu 2p XPS spectra of Ce-BPDS-Cu.

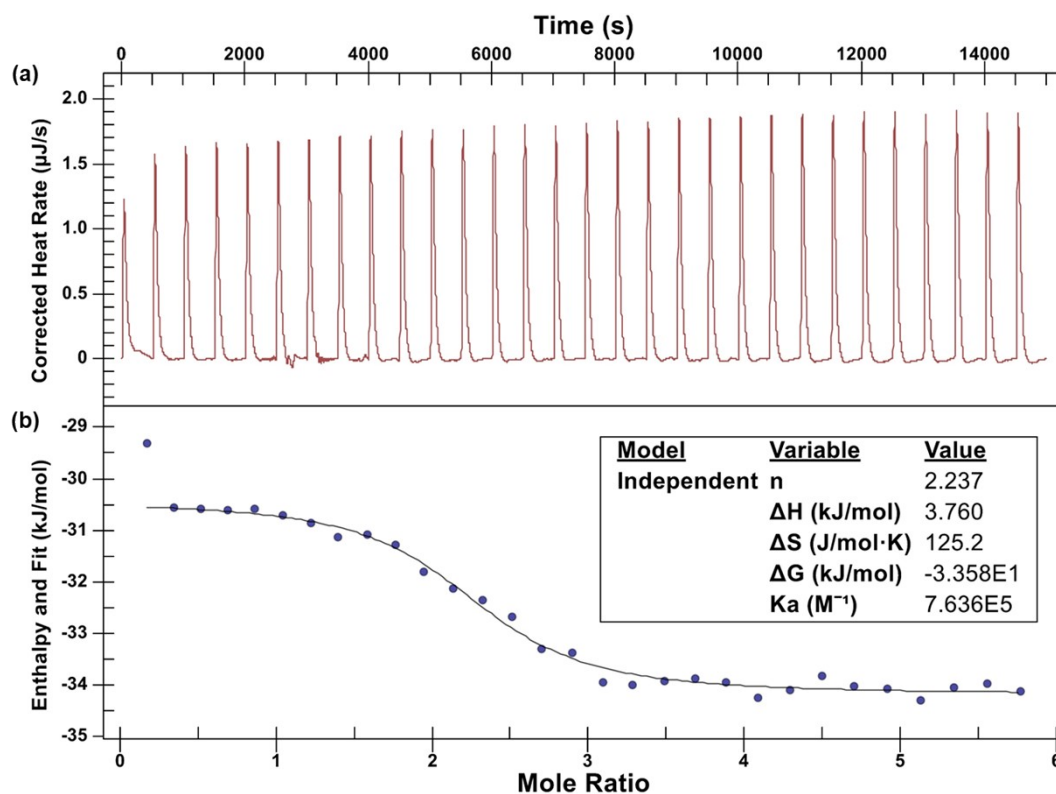
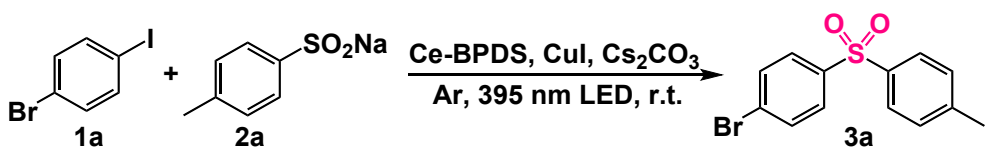


Figure S12. Microcalorimetric titration of Ce-BPDS with CuI in DMSO at 298.15K. (a) Raw data for sequential 25 injections (10 μ L per injection) of CuI solution (0.4 mM) injecting into Ce-BPDS solution (0.02 mM). (b) Apparent reaction heat obtained from the integration of calorimetric traces.

6. Data Relative to the Photocatalytic C(sp²)-S Cross-Coupling.

Table S4. The photocatalytic C(sp²)-S cross-coupling of 4-bromodiobenzene with sodium 4-methylbenzenesulfinate under different conditions^[a]



The reaction scheme shows the photocatalytic C(sp²)-S cross-coupling of 4-bromoiodobenzene (**1a**) and sodium 4-methylbenzenesulfinate (**2a**) to form 4-bromo-4'-methylbiphenyl-2-sulfone (**3a**). The reaction conditions are Ce-BPDS, CuI, Cs₂CO₃ in Ar, irradiated with a 395 nm LED at room temperature (r.t.).

Entry	Variation from the standard conditions	Yield [%] ^[b]
1	none	57
2	0.5 μmol CuI	20
3	1.5 μmol CuI	45
4	2.5 μmol CuI	38
5	3.0 μmol CuI	22

[a] Standard condition: **1a** (0.05 mmol), **2a** (0.5 mmol), Cs₂CO₃ (0.05 mmol), Ce-BPDS (0.5 μmol), CuI (1.0 μmol) and DMSO (2 mL). The mixture solution was irradiated with a 395 nm LED at room temperature in argon atmosphere for 4 hours. [b] The yields were determined by GC using 1,3,5-trimethoxybenzene as an internal standard.

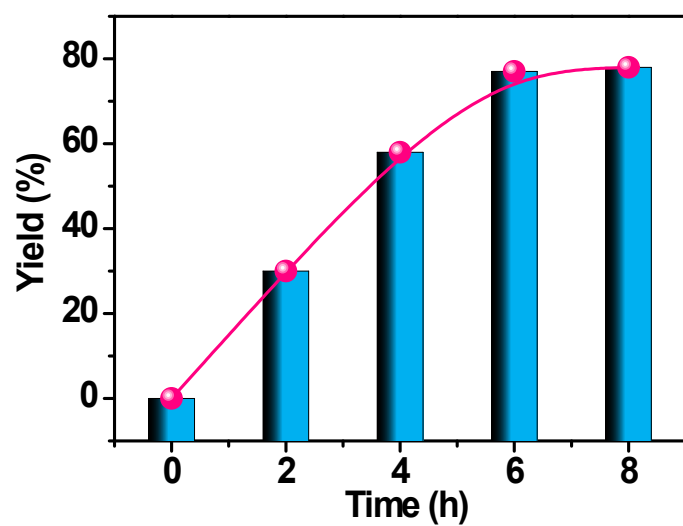


Figure S13. Yield-time plots of Ce-BPDS-Cu photocatalytic C(sp²)-S cross-coupling under the standard conditions.

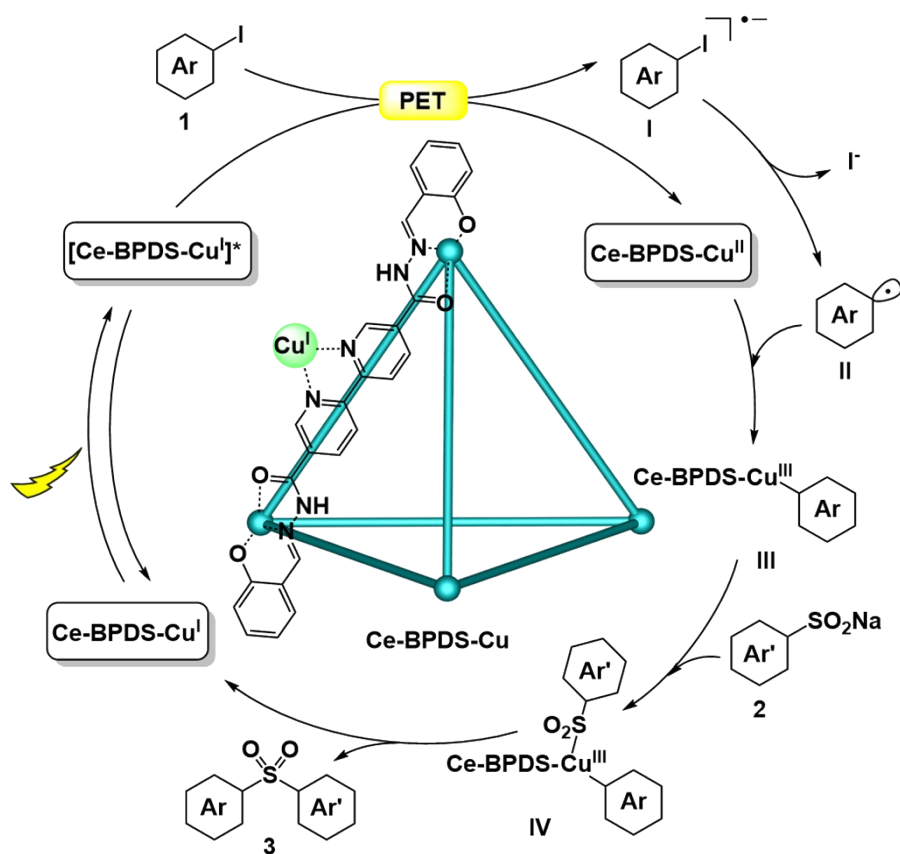
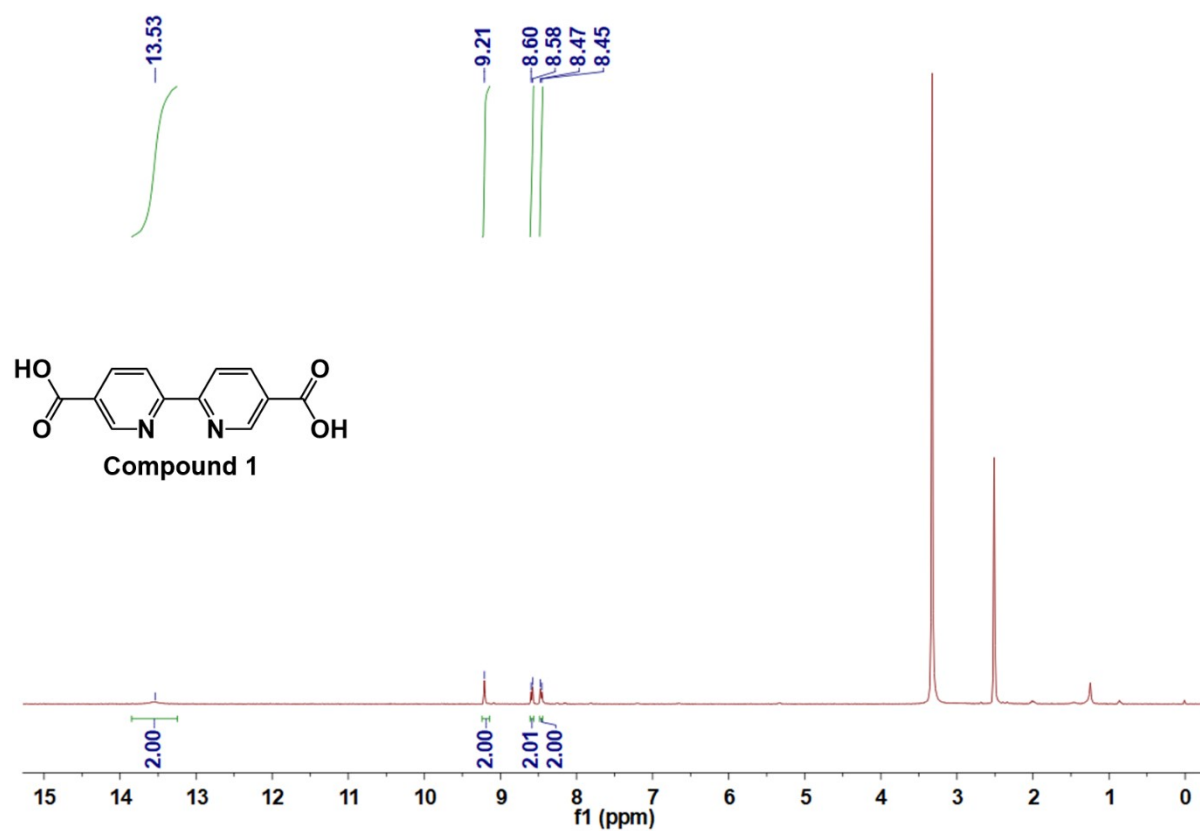
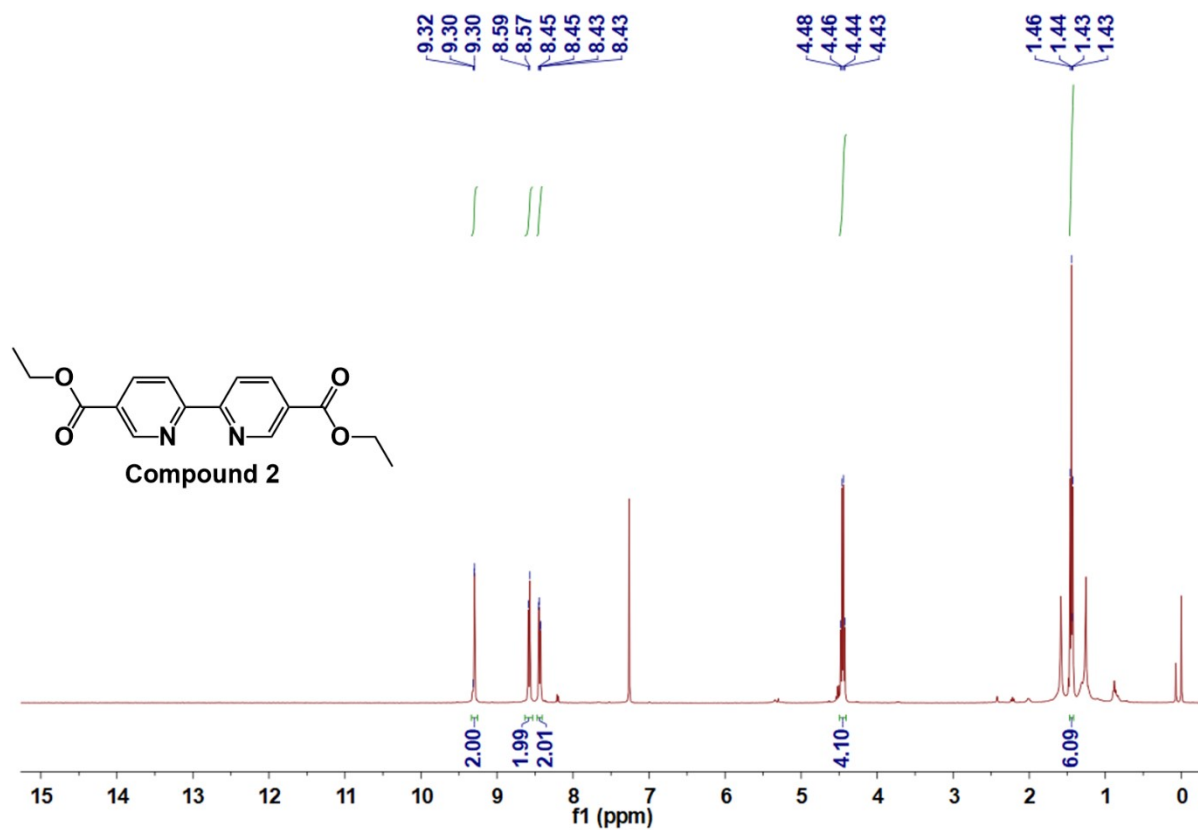


Figure S14. The proposed mechanism for the Ce-BPDS-Cu photocatalytic C(sp²)-S cross-coupling of aryl iodides and sodium benzenesulfinate.

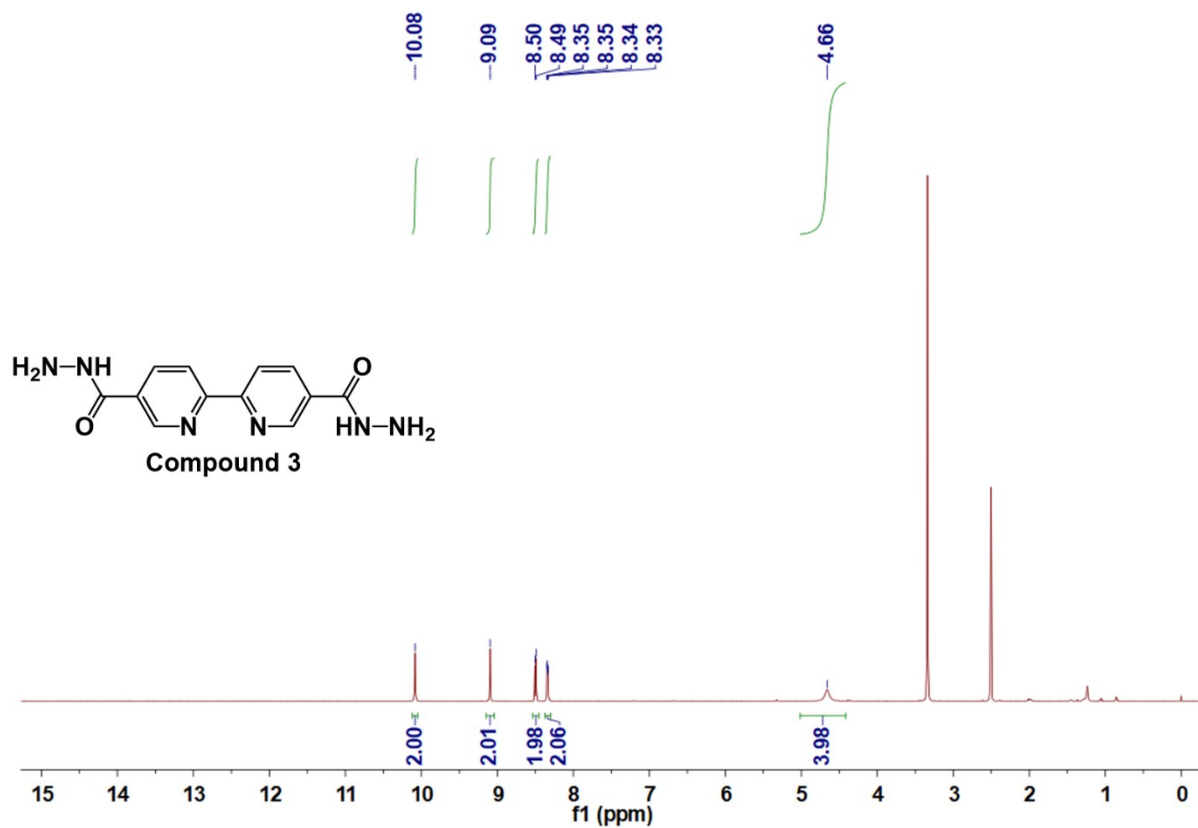
7. NMR spectra.



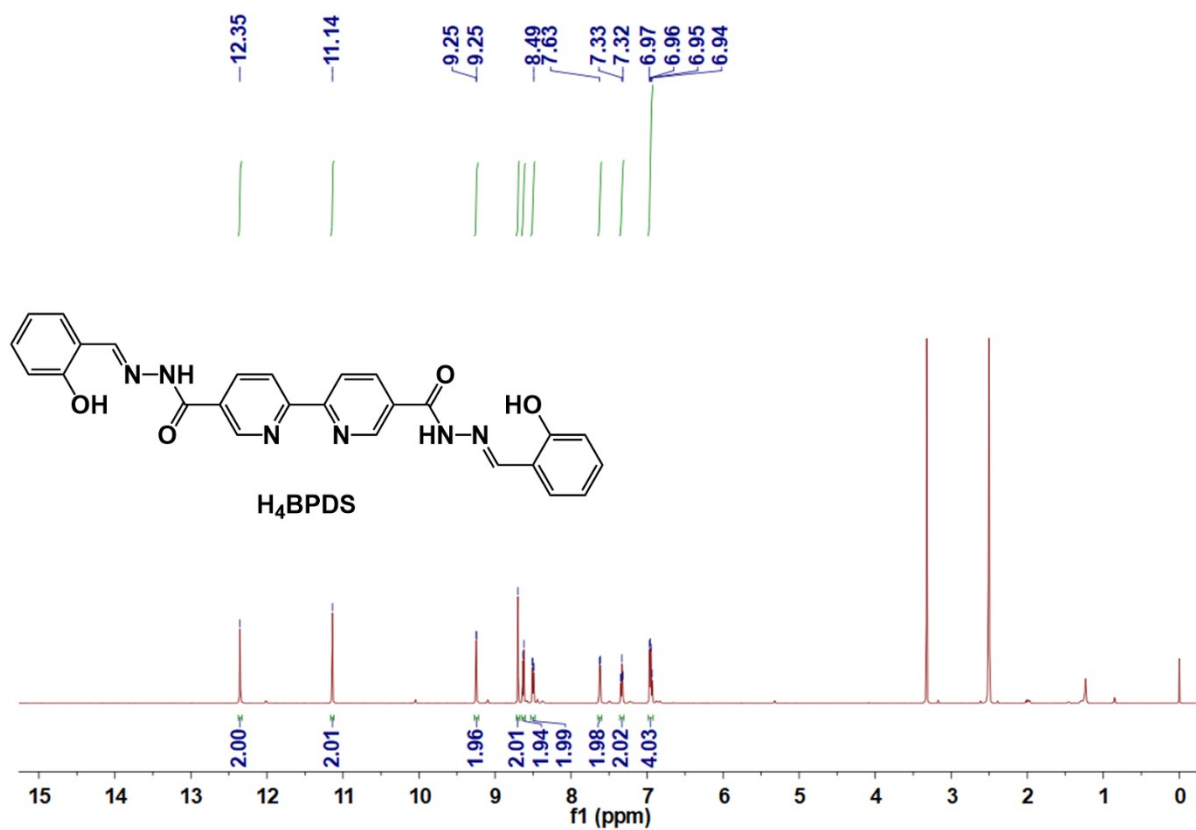
[2,2'-bipyridine]-5,5'-dicarboxylic acid (**Compound 1**): ¹H NMR (400 MHz, DMSO-*d*₆): δ 13.53 (s, 2H), 9.21 (s, 2H), 8.59 (d, *J* = 8.0 Hz, 2H), 8.46 (d, *J* = 8.0 Hz, 2H).



Diethyl [2,2'-bipyridine]-5,5'-dicarboxylate (**Compound 2**): ¹H NMR (400 MHz, CDCl₃): δ 9.29 (s, 2H), 8.58 (d, *J* = 8.4 Hz, 2H), 8.44 (d, *J* = 8.4 Hz, 2H), 4.45 (q, *J* = 3.2 Hz, 4H), 1.44 (t, *J* = 3.2 Hz, 6H).

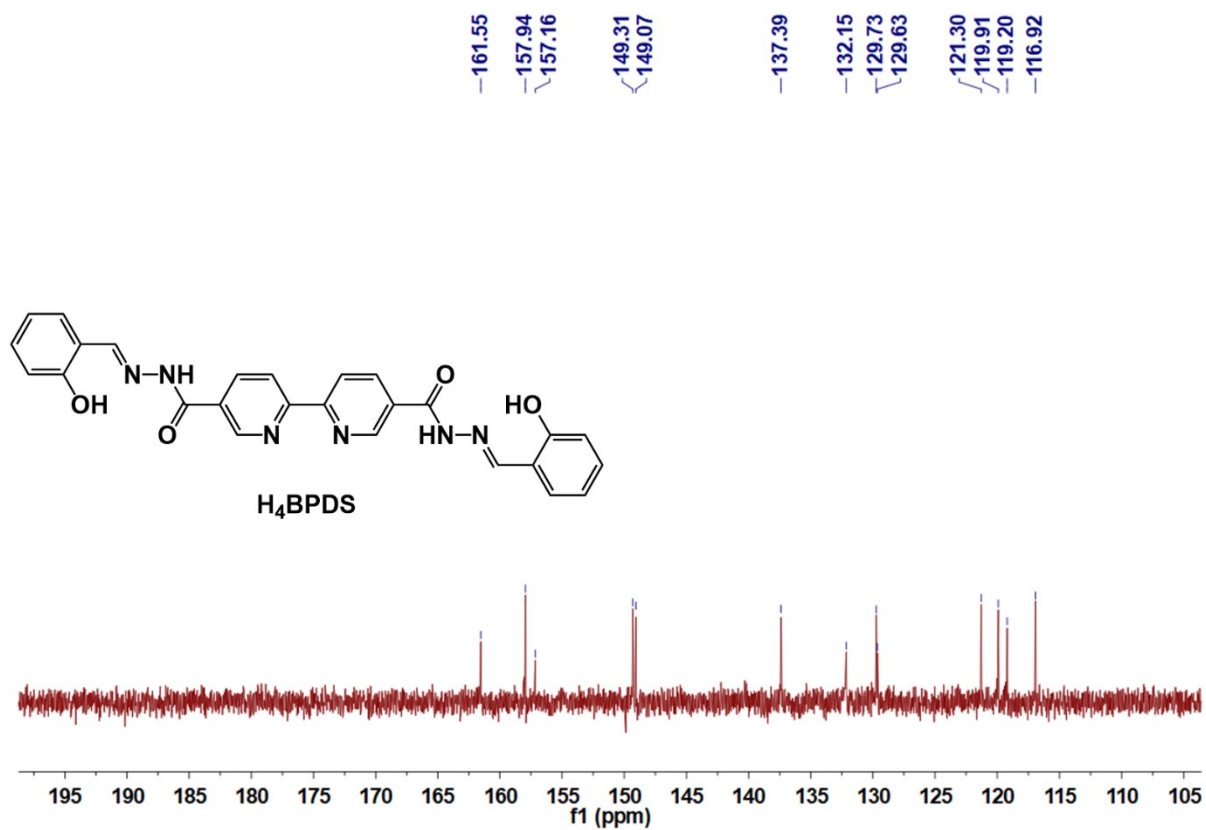


[2,2'-bipyridine]-5,5'-dicarbohydrazide (**Compound 3**): $^1\text{H NMR}$ (600 MHz, $\text{DMSO-}d_6$): δ 10.08 (s, 2H), 9.09 (s, 2H), 8.50 (d, $J = 8.4$ Hz, 2H), 8.34 (d, $J = 8.4$ Hz, 2H), 4.66 (s, 4H).



N⁵,N^{5'}-bis((E)-2-hydroxybenzylidene)-[2,2'-bipyridine]-5,5'-dicarbohydrazide (**H₄BPDS**):

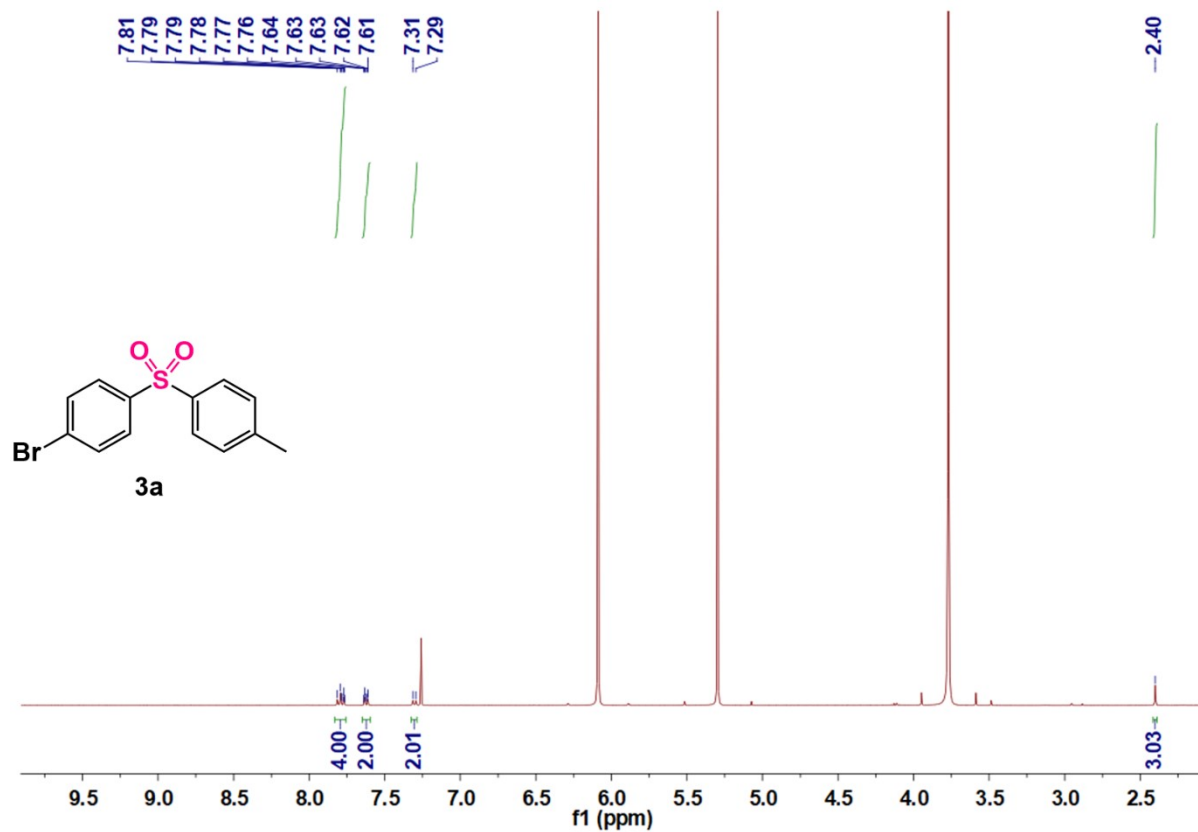
¹H NMR (600 MHz, DMSO-*d*₆): δ 12.35 (s, 2H), 11.14 (s, 2H), 9.25 (s, 2H), 8.70 (s, 2H), 8.63 (d, *J* = 8.4 Hz, 2H), 8.50 (d, *J* = 8.4 Hz, 2H), 7.62 (d, *J* = 6.6 Hz, 2H), 7.33 (t, *J* = 7.8 Hz, 2H), 6.95 (dd, *J* = 12.0, 7.8 Hz, 4H).



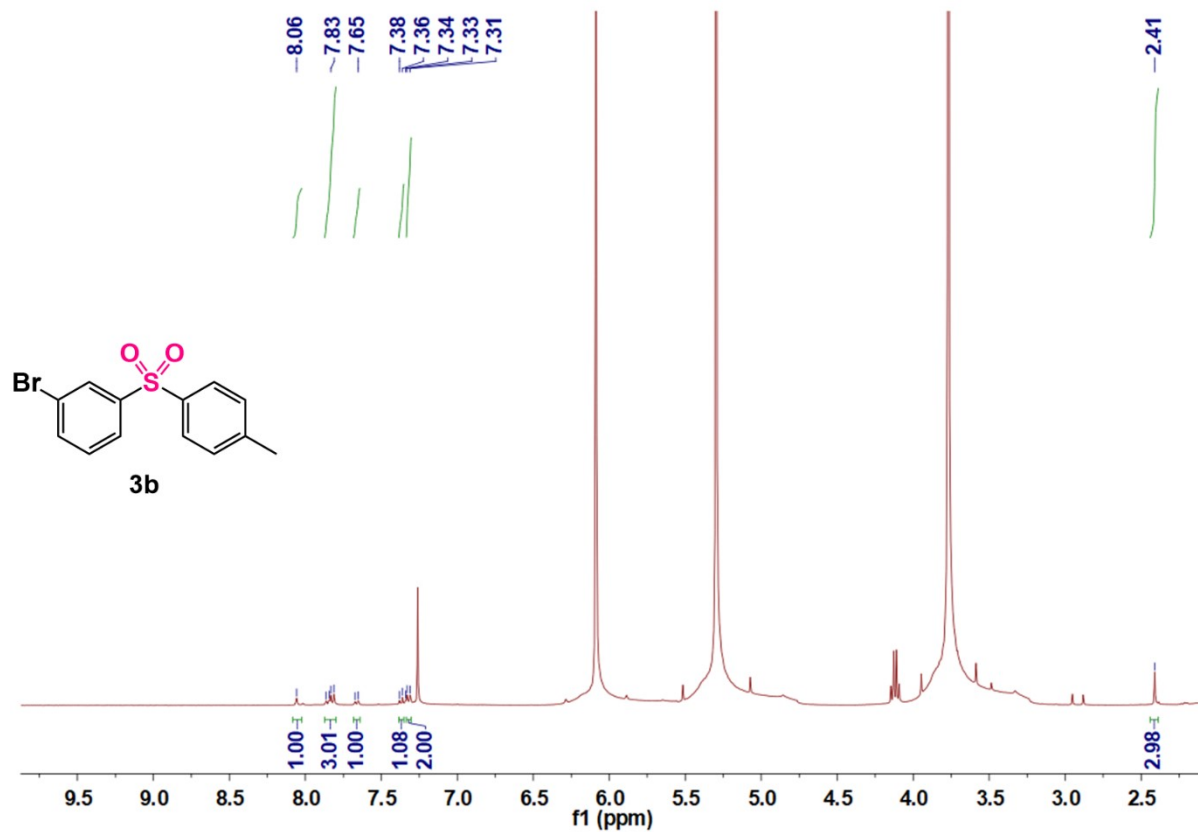
$N^{5},N^{''5}$ '-bis((E)-2-hydroxybenzylidene)-[2,2'-bipyridine]-5,5'-dicarbohydrazide (**H₄BPDS**):

^{13}C NMR (101 MHz, $\text{DMSO-}d_6$): δ 161.6, 157.9, 157.2, 149.3, 149.0, 137.4, 132.2, 129.7,

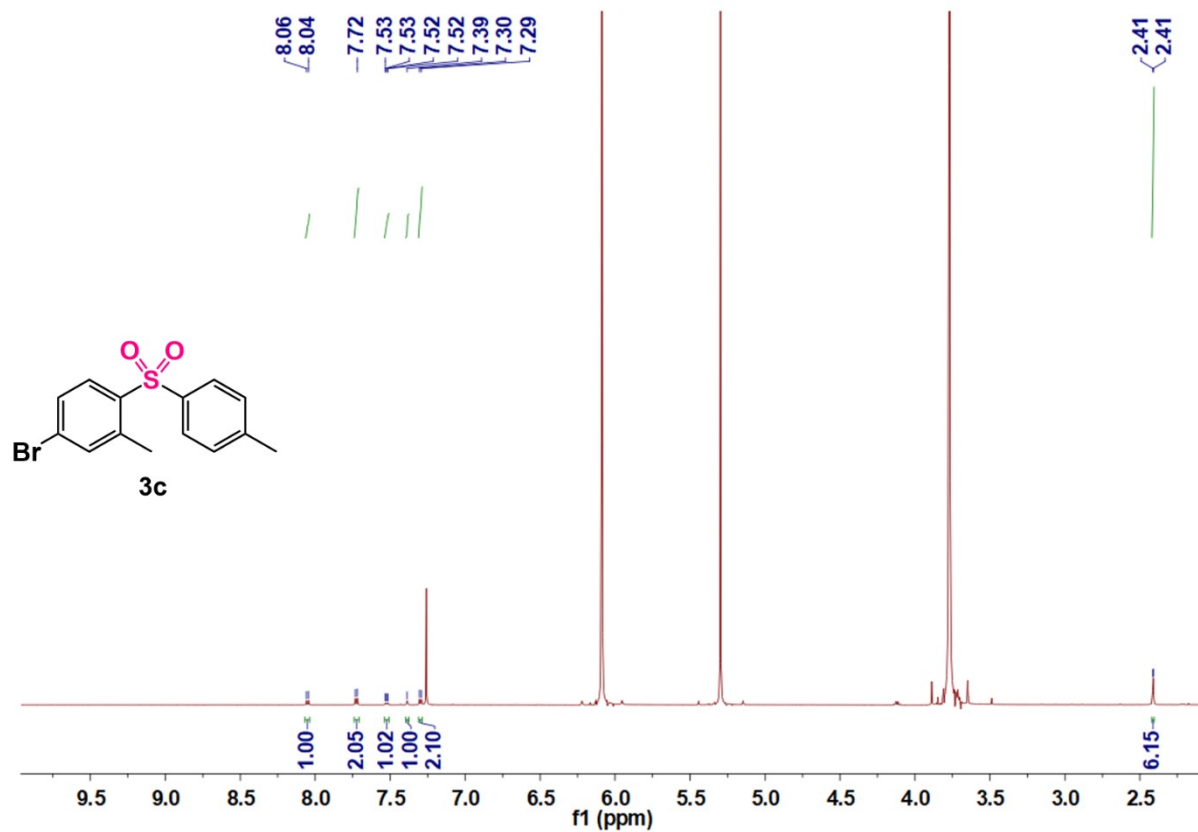
129.6, 121.3, 119.9, 119.2, 116.9.



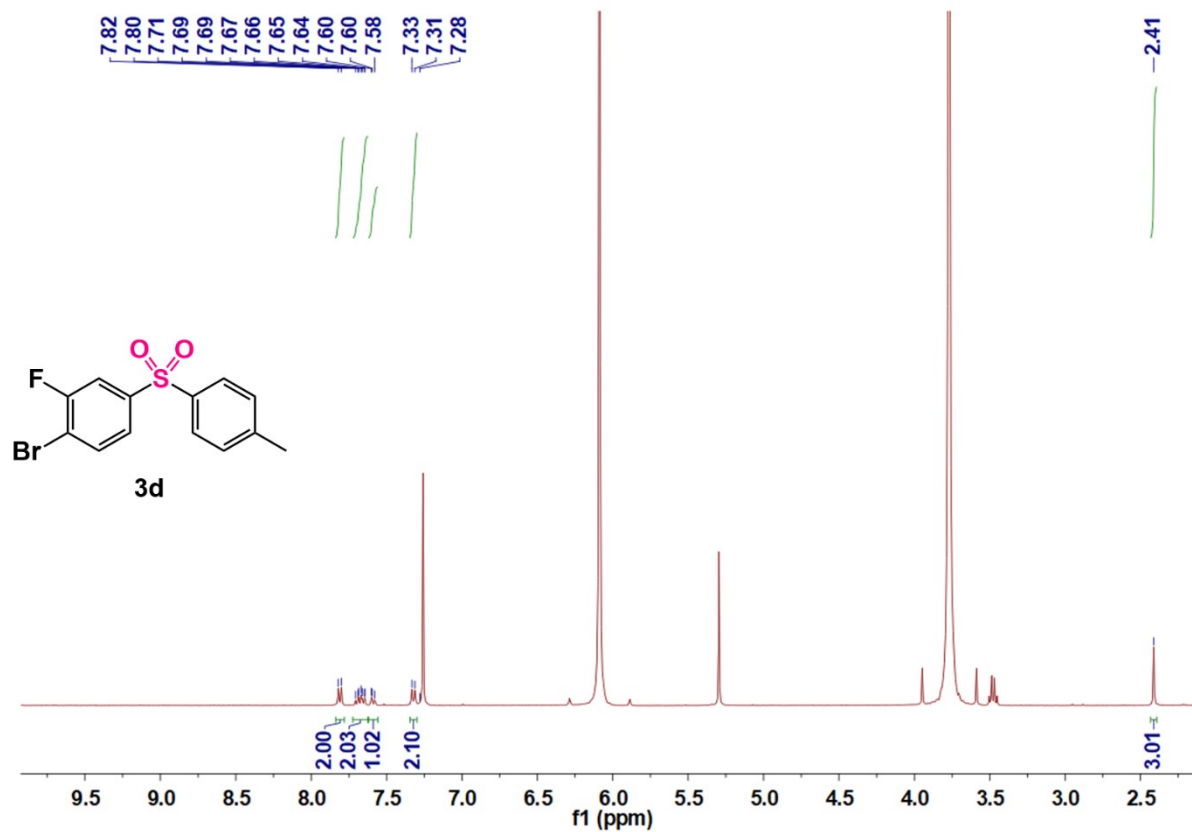
4-Bromophenyl 4-methylphenyl sulfone (**3a**): ¹H NMR (400 MHz, CDCl₃): δ 7.82 – 7.75 (m, 4H), 7.65 – 7.60 (m, 2H), 7.30 (d, *J* = 8.0 Hz, 2H), 2.40 (s, 3H).



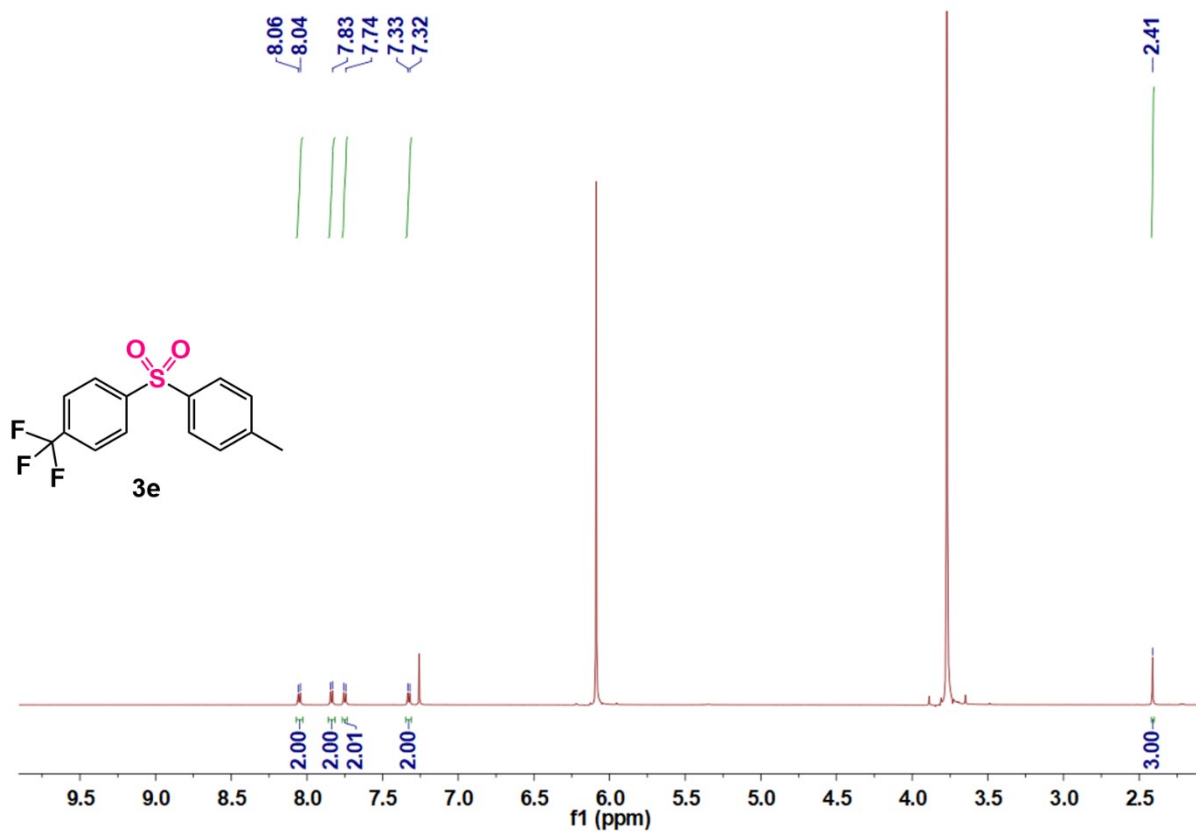
1-Bromo-3-[(4-methylphenyl)sulfonyl]benzene (**3b**): ¹H NMR (400 MHz, CDCl₃): δ 8.06 (s, 1H), 7.84 (dd, *J* = 12.4, 8.4 Hz, 3H), 7.66 (d, *J* = 8.0 Hz, 1H), 7.37 (d, *J* = 8.0 Hz, 1H), 7.32 (d, *J* = 8.0 Hz, 2H), 2.41 (s, 3H).



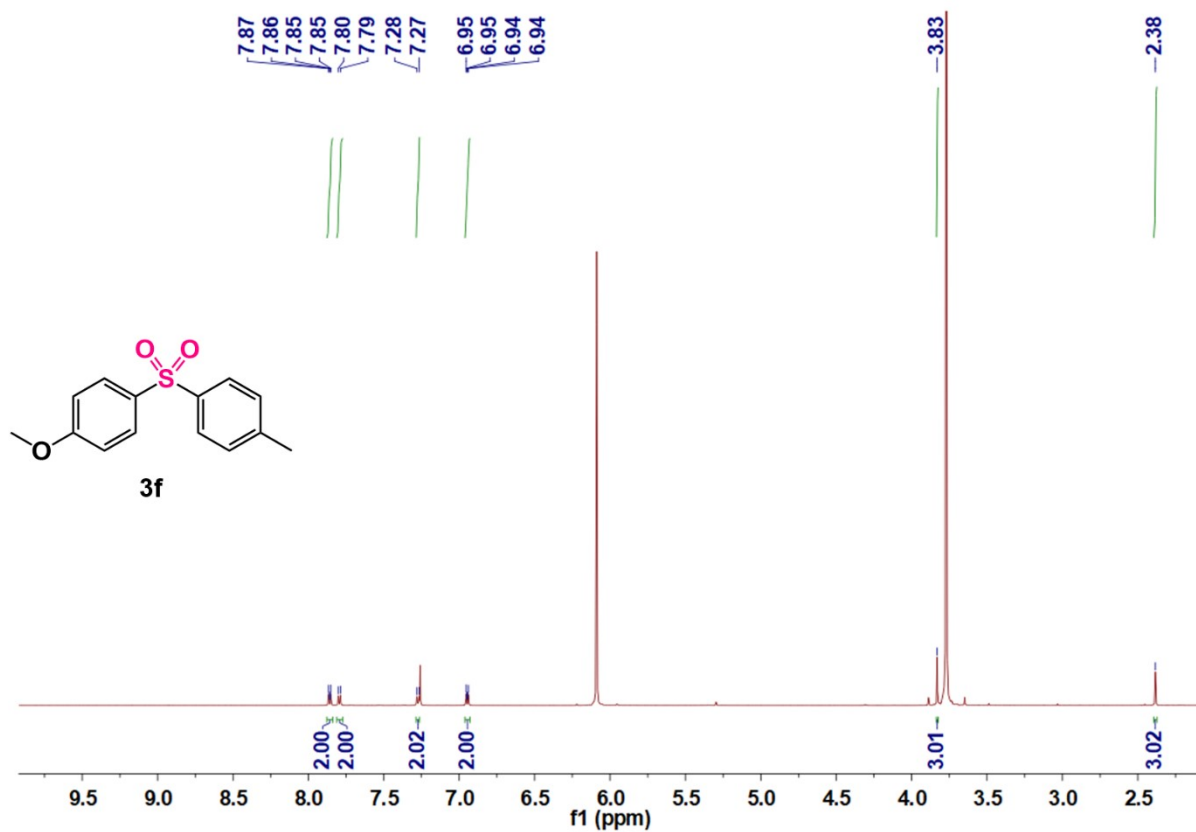
4-Bromo-2-methyl-1-[(4-methylphenyl)sulfonyl]benzene (**3c**): ¹H NMR (600 MHz, CDCl₃): δ 8.05 (d, *J* = 8.4 Hz, 1H), 7.73 (d, *J* = 8.4 Hz, 2H), 7.52 (dd, *J* = 8.4 Hz, *J* = 1.8 Hz, 1H), 7.39 (s, 1H), 7.30 (d, *J* = 8.4 Hz, 2H), 2.41 (d, *J* = 1.8 Hz, 6H).



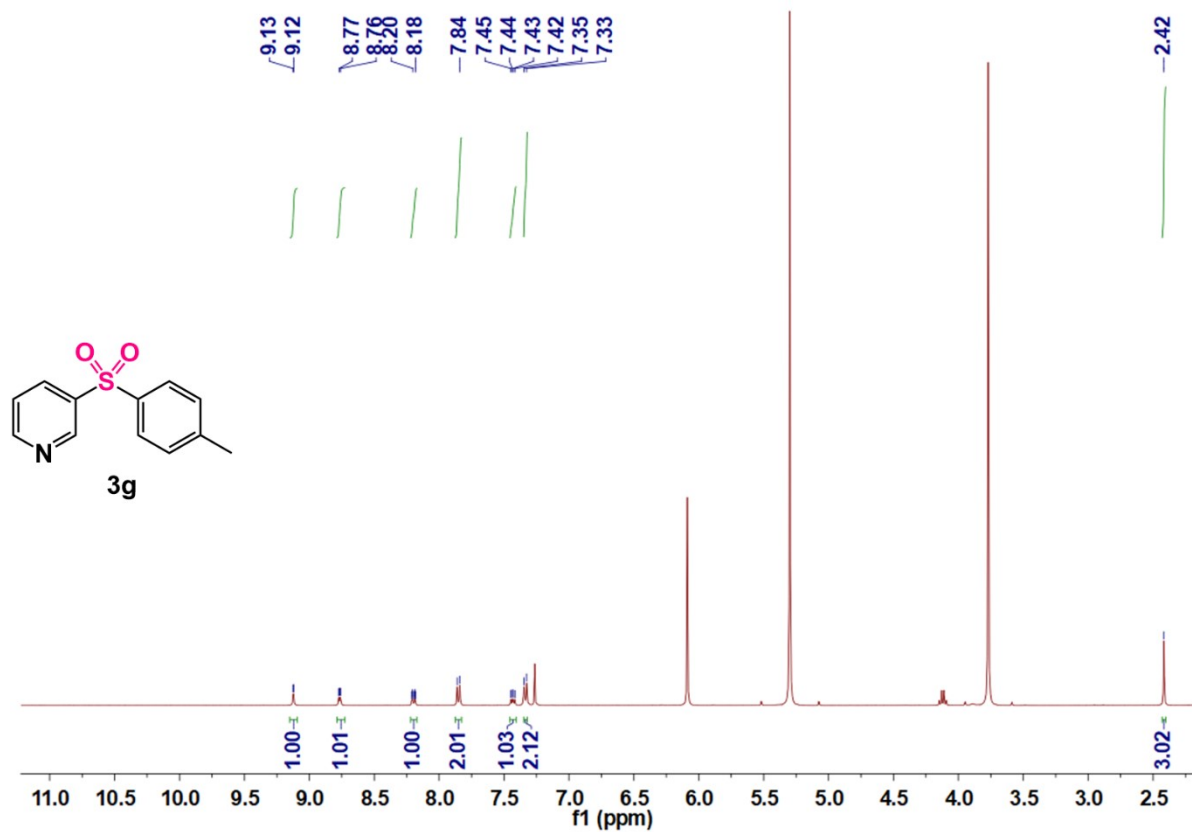
4-Bromo-3-fluorophenyl-1-[(4-methylphenyl)sulfonyl]benzene (**3d**): ¹H NMR (400 MHz, CDCl₃): δ 7.81 (d, *J* = 8.4 Hz, 2H), 7.59 (d, *J* = 8.4 Hz, 2H), 7.59 (d, *J* = 8.4 Hz, 1H), 7.31 (d, *J* = 8.0 Hz, 2H), 2.41 (s, 3H).



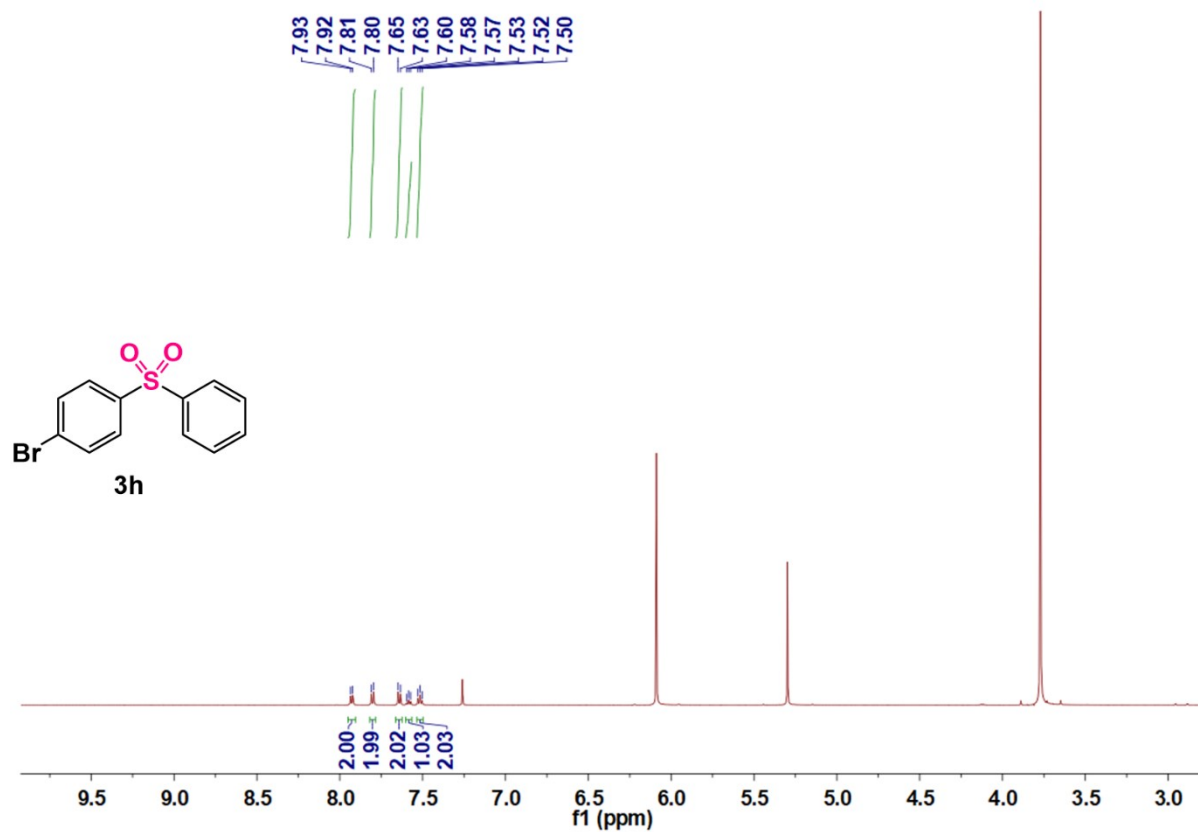
1-[(4-Methylphenyl)sulfonyl]-4-(trifluoromethyl)benzene (**3e**): ¹H NMR (600 MHz, CDCl₃):
 δ 8.05 (d, $J = 7.8$ Hz, 2H), 7.84 (d, $J = 8.4$ Hz, 2H), 7.75 (d, $J = 8.4$ Hz, 2H), 7.33 (d, $J = 7.8$
 Hz, 2H), 2.41 (s, 3H).



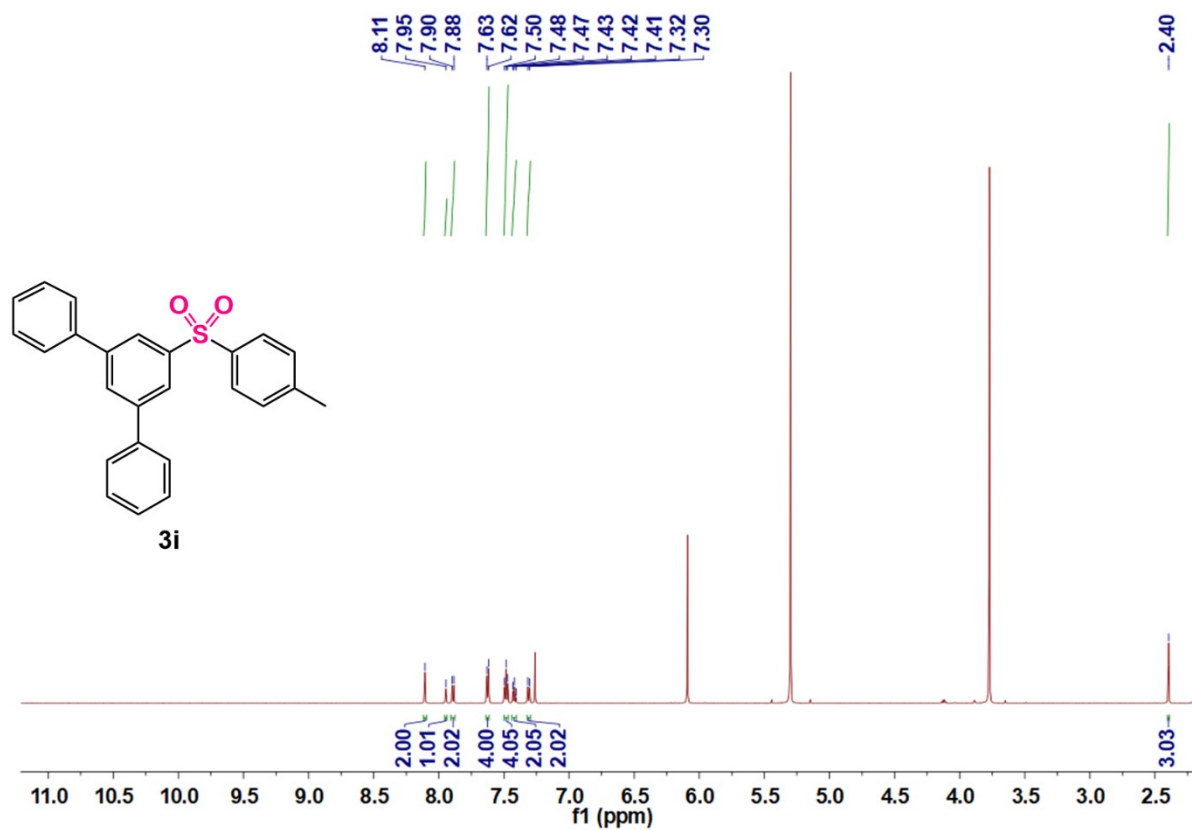
1-Methoxy-4-[(4-methylphenyl)sulfonyl]benzene (**3f**): ¹H NMR (600 MHz, CDCl₃): δ 7.86 (d, *J* = 9.0 Hz, 2H), 7.79 (d, *J* = 7.8 Hz, 2H), 7.27 (d, *J* = 7.8 Hz, 2H), 6.95 (d, *J* = 9.0 Hz, 2H), 3.83 (s, 3H), 2.38 (s, 3H).



3-[(4-Methylphenyl)sulfonyl]pyridine (**3g**): ¹H NMR (400 MHz, CDCl₃): δ 9.12 (s, 1H), 8.77 (d, *J* = 4.8 Hz, 1H), 8.19 (d, *J* = 8.0 Hz, 1H), 7.85 (d, *J* = 8.4 Hz, 2H), 7.43 (dd, *J* = 8.0, 4.8 Hz, 1H), 7.34 (d, *J* = 8.4 Hz, 2H), 2.42 (s, 3H).



1-Bromo-4-(phenylsulfonyl)benzene (**3h**): ¹H NMR (600 MHz, CDCl₃): δ 7.93 (d, J = 7.8 Hz, 2H), 7.80 (d, J = 9.0 Hz, 2H), 7.64 (d, J = 9.0 Hz, 2H), 7.58 (t, J = 7.2 Hz, 1H), 7.52 (t, J = 7.8 Hz, 2H).



5'-[(4-Methylphenyl)sulfonyl]-1,1':3',1''-terphenyl (**3i**): ¹H NMR (600 MHz, CDCl₃): δ 8.11 (s, 2H), 7.95 (s, 1H), 7.89 (d, *J* = 5.6 Hz, 2H), 7.62 (d, *J* = 4.8 Hz, 4H), 7.48 (t, *J* = 4.8 Hz, 4H), 7.42 (t, *J* = 4.8 Hz, 2H), 7.31 (d, *J* = 5.6 Hz, 2H), 2.40 (s, 3H).

8. References.

- S1. Duan, H.; Li, M.; Zhang, G.; Gallagher, J.; Huang, Z.; Sun, Y.; Luo, Z.; Chen, H.; Miller, J.; Zou, R.; Lei, A.; Zhao, Y. Single-Site Palladium(II) Catalyst for Oxidative Heck Reaction: Catalytic Performance and Kinetic Investigations. *ACS Catal.* **2015**, *5*, 3752–3759.
- S2. Wang, J.; Zhang, J.; Peh, S.; Liu, G.; Kundu, T.; Dong, J.; Ying, Y.; Qian, Y.; Zhao, D. Cobalt-containing covalent organic frameworks for visible light-driven hydrogen evolution. *Sci. China Chem.* **2020**, *63*, 192–197.
- S3. SMART Data Collection Software, version 5.629; Bruker AXS Inc.: Madison, WI, 2003.
- S4. SAINT Data Reduction Software, version 6.54; Bruker AXS Inc.: Madison, WI, 2003.
- S5. Dolomanov, O. V.; Bourhis, L. J.; Gildea, R. J.; Howard, J. A. K.; Puschmann, H. *OLEX2*: A Complete Structure Solution, Refinement and Analysis Program. *J. Appl. Crystallogr.* **2009**, *42*, 339–341.
- S6. Sheldrick, G. M. Crystal Structure Refinement with *SHELXL*. *Acta. Crystallogr. C Struct. Chem.* **2015**, *71*, 3–8.
- S7. Sheldrick, G. M. *SHELXT* - Integrated Space-Group and Crystal-Structure Determination. *Acta. Crystallogr. A Found. Adv.* **2015**, *71*, 3–8.
- S8. Spek, A. L. Single-crystal structure validation with the program *PLATON*. *J. Appl. Cryst.* **2003**, *36*, 7–13.